Available online at www.sciencedirect.com

SciVerse ScienceDirect

Ceramics International 39 (2013) 7407–7414

CERAMICS INTERNATIONAL

www.elsevier.com/locate/ceramint

Effect of amine and carboxyl functionalization of sub-micrometric MCM-41 spheres on controlled release of cisplatin

C.O. Arean[a], M.J. Vesga[a], J.B. Parra[b], M.R. Delgado[a,*]

[a]*Department of Chemistry, University of the Balearic Islands, 07122 Palma de Mallorca, Spain*
[b]*Instituto Nacional del Carbón, CSIC, 33080 Oviedo, Spain*

Received 30 January 2013; accepted 25 February 2013
Available online 7 March 2013

Abstract

Mesoporous MCM-41 type silica spheres having a sub-micrometer size were synthesized following an adaptation of Stöber's method. This parent material was then functionalized with 3-aminopropyl triethoxysilane and with 3-propanonitrile triethoxysilane, followed by oxidation of the cyano-group to the corresponding carboxy-group. After proper characterization, the samples were loaded with cisplatin and subjected to in vitro tests in order to obtain the corresponding drug release profile. The carboxy-functionalized MCM-41 sample was found to show a release kinetics that should facilitate controlled drug delivery over a significantly larger time period (about 140 h) than both, unmodified MCM-41 and amino-functionalized MCM-41 samples.

Keywords: Drug delivery; Cisplatin; MCM-41; Mesoporous materials

1. Introduction

Cisplatin, *cis*-diamminedichloroplatinum(II), is currently used, either on its own or combined with other therapeutic drugs, for the treatment of testicular [1,2], ovarian [3,4], cervical [5,6] and lung [7,8] cancers, as well as malignant mesothelioma [9,10] and other carcinomas. Nevertheless, a main problem with cancer therapy using cisplatin is to keep adverse side effects under control. The high nephrotoxicity of cisplatin can potentially cause kidney failure, and the drug is also known to show distinctive dose related ototoxicity [11–14] hence the convenience to search for controlled drug delivery systems able to improve drug pharmacodynamics and minimize adverse collateral effects.

Many current studies on potential carriers for controlled drug delivery focus on polymers [15,16], liposomes [17,18] and porous inorganic solids [19–22]; among the latter, ordered mesoporous silica of the MCM-41 and SBA type are receiving the largest attention [23–32]. Main reasons for that are (i) these materials show a large specific pore volume made up of regular pores having a diameter in the nanometer range, which facilitates controlled delivery of the pharmaceutical drug, and (ii) the internal surface of pores can be functionalized with several kinds of organic molecules that can modulate physical or chemical interactions between the drug and the carrier [25,33,34], thus facilitating control over the kinetics of drug delivery; these features should help to maintain the therapeutic drug level for an extended time period while minimizing undesirable high peaks of drug concentration immediately following administration. It should be added that both, silica xerogels and mesoporous silica particles were reported to display low toxicity and reasonably good biocompatibility when used as drug carriers [35–38].

Herein, we report on the uptake and the kinetics of in vitro cisplatin release by MCM-41 mesoporous silica prepared in the form of sub-micrometric spheres having a diameter in the range of 700–870 nm. Besides pure MCM-41, comparative studies were also carried out on functionalized samples. Both, amino and carboxy functionalized MCM-41 samples were investigated. Characterization of the solids was attained by means of powder X-ray diffraction, scanning electron

*Corresponding author. Tel.: +34 971172633; fax: +34 971173426.
E-mail address: montserrat.rodriguez@uib.es (M.R. Delgado).

0272-8842/$ - see front matter © 2013 Elsevier Ltd and Techna Group S.r.l. All rights reserved.
http://dx.doi.org/10.1016/j.ceramint.2013.02.084

microscopy, solid state MAS NMR and nitrogen adsorption–desorption isotherms at −196 °C. In vitro drug delivery kinetics was monitored by means of quantitative colorimetric assays with *o*-phenylendiamine. Note that a main reason for using sized controlled MCM-41 sub-micrometric spheres (instead of irregularly shaped MCM-41 xerogels) as potential drug carriers was to render the results obtained for the different samples more directly comparable. Regarding functionalization, amino and carboxyl groups were chosen on account of the expected difference in their interaction energy with cisplatin; similar functionalization of MCM-41 was frequently reported in the literature related to mesoporous silicas as controlled drug delivery carriers [39–41].

2. Experimental

2.1. Synthesis of MCM-41 spheres

Mesoporous MCM-41 silica spheres were synthesized according to the procedure described by Manzano et al. [42] which follows a variation of Stöber's method [43,44]. The synthesis procedure was as follows. 2.4 g of hexadecyltrimethyl ammonium bromide (99%, Aldrich) was dissolved in 420 ml of water. To this solution 730 ml of ethanol (96%, Scharlau) and 180 ml of ammonia (25%, Fluka) were added. After stirring for 15 min, 10 ml of tetraethyl orthosilicate (98%, Aldrich) was dropwise added and the mixture was kept under stirring for 2 h at 35 °C. The solid product obtained was filtered, thoroughly washed with distilled water and ethanol and air-dried in a desiccator. In order to remove the surfactant, the powder was then heated at 550 °C, first under a nitrogen flow for 3 h and then in air for another 3 h. Complete removal of the surfactant was checked by means of infrared spectroscopy and thermogravimetry, which did not reveal presence of any residual organic species.

2.2. Functionalization of MCM-41 spheres

Amino-functionalized MCM-41 spheres (NH_2-MCM-41) were prepared by treating MCM-41 with 3-aminopropyl triethoxysilane (99%, Fluka) as follows. Template-free MCM-41 spheres were dehydrated at 80 °C for 2 h under a nitrogen flow and then refluxed with 5 mmol of APTES per gram of SiO_2 in toluene (40 ml of toluene per gram of SiO_2) for 24 h. The obtained product was filtered, washed with a 1:1 mixture of diethyl ether and dichloromethane and finally dried in a desiccator.

Carboxy-functionalized MCM-41 spheres were prepared by a two-step procedure. First, MCM-41 spheres were sylilated with 3-propanonitrile triethoxysilane (97%, Fluka) following a procedure similar to that described for the NH_2-MCM-41 sample. From the thus obtained cyano-functionalized MCM-41, the carboxy-functionalized derivative (COOH-MCM-41) was obtained by acid-catalyzed oxidation of the cyano-group by refluxing the solid in an aqueous 12% solution of HCl for 3 h.

2.3. Materials characterization

Several instrumental techniques were used for sample characterization. Small angle X-ray diffraction patterns were recorded on a Siemens D5000 diffractometer, equipped with CuKα radiation ($\lambda = 1.5406$ Å). The diffractograms were recorded by step scanning over the range 1–10° (2θ) with a step size of 0.01° and an accumulation time of 2 s. Particle morphology was analyzed by scanning electron microscopy using a Hitachi S-3400N microscope operated at 15 kV. Surface area and porosity were determined from nitrogen adsorption–desorption isotherms obtained (at −196 °C) on a Micromeritics Tristar II 3020 analyzer. In all cases, the solid was degassed at 120 °C for 6 h under vacuum (residual pressure $< 10^{-5}$ mbar) before nitrogen adsorption. Solid-state ^{29}Si cross-polarized NMR spectra were recorded at room temperature on a Bruker Avance III 600 spectrometer operated at 119.22 MHz, with a pulse width of 6.1 μs and a recycle delay of 60 s. Solid-state NMR spectroscopy was used as a direct proof of MCM-41 functionalization. The peaks at around −92, −100 and −110 ppm should be attributed to Q^2, Q^3 and Q^4 ($Q^n = Si(OSi)_n(OH)_{4-n}$) silicon atoms, respectively, whereas those at around −58 and −70 ppm are attributed to T^2 and T^3 ($T^n = R\text{-}Si(OSi)_n(OH)_{3-n}$) silicon atoms, respectively, which signal the presence of Si–C bonds [45,46]. Fourier transform infrared spectroscopy was performed on a Bruker IFS66 spectrometer using the KBr pellet method. Cisplatin uptake and release was monitored by UV spectrometry at 706 nm using a UV–vis Varian Cary 300 Bio spectrometer, as described below.

2.4. Cisplatin loading and release measurements

MCM-41, NH_2-MCM-41 and COOH-MCM-41 samples were loaded with cisplatin (99.5%, Aldrich) by immersing them into a water solution of cisplatin (1 mg ml^{-1}) kept under vigorous magnetic stirring for 24 h at 37 °C. A 1:10 (by weight) ratio of cisplatin to solid sample was used. The cisplatin loaded samples, hereafter termed MCM-41C, NH_2-MCM-41C and COOH-MCM-41C, were recovered by filtration, washed with distilled water and left to dry in a desiccator.

The in vitro drug delivery assays were performed by immersing 100 mg of each cisplatin loaded sample into 50 ml of a 0.9% NaCl aqueous solution at 37 °C, which was maintained with continuous stirring. An aliquot of the solution was taken at regular time intervals and analyzed for cisplatin content (after centrifuging to have a clear solution). In order to keep a constant volume, saline solution was added (each time) to compensate for the volume of liquid taken out.

Cisplatin concentration was determined by the *o*-phenyl enediamine (OPDA) colorimetric assay described by Golla

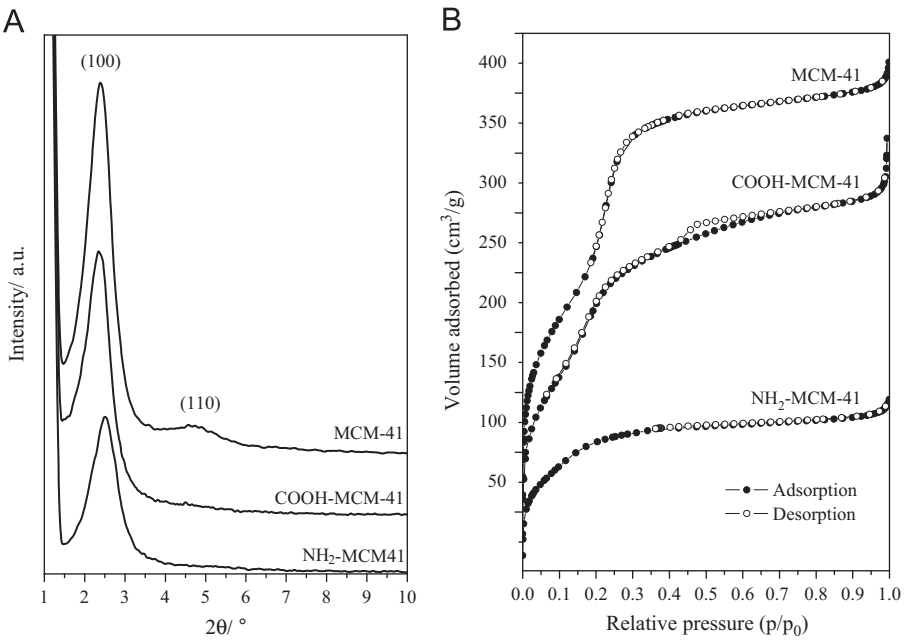

Fig. 1. (A) X-ray diffractograms (CuKα radiation) of MCM-41, NH_2-MCM-41 and COOH-MCM-41 samples. (B) Nitrogen adsorption–desorption isotherms at −196 °C on the same samples.

and Ayres [47]. A solution of OPDA in N,N-dimethylformamide (1.6 mg ml^{-1}) was prepared, to this solution an equal volume of the cisplatin solution being tested was added, and the resulting solution was heated at 90°C for 30 min. Aliquots were then analyzed by UV–visible spectroscopy at 706 nm. Calibration curves were obtained using standard solutions of cisplatin in the loading medium (H_2O) and in the release medium (0.9% NaCl), as both media and sodium chloride concentration were found to have an effect on the assay. The linear ranges for this assay were found to be 0.5–7.0 μg ml^{-1} (cisplatin in H_2O) and 0.5–16.0 μg ml^{-1} (cisplatin in 0.9% NaCl).

3. Results and discussion

3.1. Characterization of the MCM-41 materials

Representative small angle X-ray diffraction patterns of the samples are shown in Fig. 1A. Pure MCM-41 shows the characteristic (100) and (110) diffraction peaks of this ordered mesoporous material [48]. The ordered mesoporous structure is basically preserved after both, amine and carboxyl functionalization (samples NH_2-MCM-41 and COOH-MCM-41, respectively). However, compared to the parent material some broadening and decreased intensity of the (100) diffraction peak is observed, as well as disappearance of the (110) peak. Similar changes, which reveal some lost of order upon functionalization of MCM-41, were reported very frequently in the related literature [40,49–51].

Fig. 1B depicts the nitrogen adsorption–desorption isotherms at −196 °C of the samples under study. The isotherm corresponding to the non-functionalized MCM-41 sample shows (as expected) the typical step in the 0.1–0.3 relative pressure (p/p_0) range, which is characteristic of an ordered mesoporous lattice [52,53]. The isotherms of the samples COOH-MCM-41 and NH_2-MCM-41 show increasingly less defined steps, in consonance with the partial loss of order already observed in the corresponding X-ray diffraction patterns. It should be noted that this is typical of organic functionalized MCM-41 silicas, which usually show a decreased order as compared to that shown by the parent material [42,45]. From the corresponding nitrogen sorption isotherms, specific (BET) surface area, pore diameter and total pore volume were calculated, using the non-local DFT method [54] for textural analysis. Results are summarized in Table 1. After amine and carboxyl functionalization a significant decrease in the total volume of adsorbed nitrogen (V_P) was observed (Fig. 1B and Table 1), and there is also a corresponding decrease of pore diameter (D_P) and specific surface area (Table 1). These observed facts are consistent with the grafting of the organic moiety to the internal pore wall, which leads (as expected) to less available space for adsorbed nitrogen.

Table 1
Textural data for MCM-41, NH_2-MCM-41 and COOH-MCM-41 samples, and corresponding uptake of cisplatin.

Sample	S_{BET} (m^2/g)	D_P (nm)	V_P (cm^3/g)	*mg cisplatin / g sample*
MCM-41	901	3.1	0.603	8.7(±0.7)
NH_2-MCM-41	389	2.4	0.186	61.4(±4.6)
COOH-MCM-41	678	2.8	0.452	14.7(±0.6)

SEM images, depicted in Fig. 2, show that samples MCM-41, NH_2-MCM-41 and COOH-MCM-41, consist of

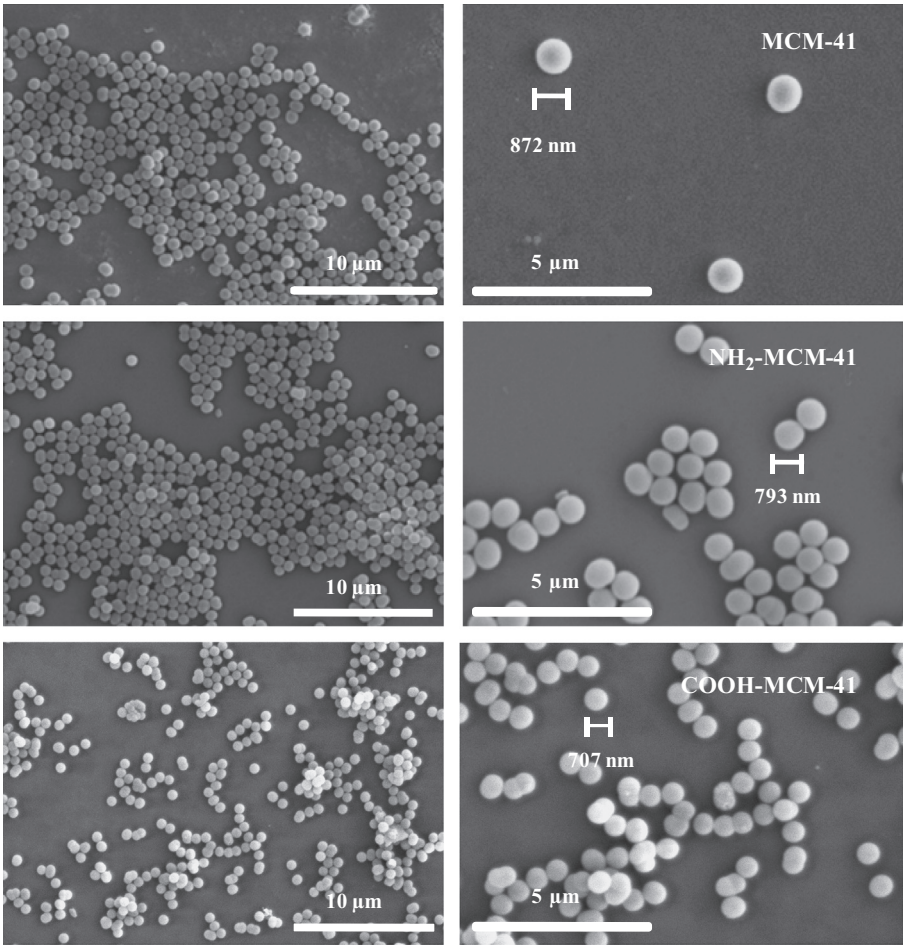

Fig. 2. Scanning electron micrographs of MCM-41, NH_2-MCM-41 and COOH-MCM-41 samples showing spherical shape. The mean particle diameter is shown in the micrographs.

microsized spheres; their corresponding diameter distribution was found to be very narrow, centered at 872, 793 and 707 nm, respectively. Statistical analysis of SEM micrographs (200 spheres were counted for each sample) showed that 95% of the micro-spheres were within the following size distribution limits: MCM-41, 872($\pm$49) nm; NH_2-MCM-41, 793($\pm$40) nm and COOH-MCM-41, 707($\pm$54) nm.

The organic functionalization of the MCM-41 samples was confirmed by ^{29}Si MAS NMR spectroscopy. Fig. 3 shows ^{29}Si NMR spectra of unmodified, amino and carboxy functionalized MCM-41 materials. Before functionalization the most intense peak is Q^3 (at ca. -101.3 ppm) which suggests that the predominant silicon species are $(SiO)_3Si–OH$, as expected for MCM-41 type silica. After functionalization (samples NH_2-MCM-41 and COOH-MCM-41) the relative intensity of the Q^2, Q^3 and Q^4 peaks changes till a different extent, depending on the sample being considered. In particular, the Q^3 and Q^2 peaks are distinctively more intense in the spectrum of the carboxy-functionalized sample as compared to that of NH_2-MCM-41. These facts can be explained on account of partial hydrolysis of siloxane bridges that is very likely to take place during the process of acid catalyzed oxidation of the cyano-functionalized precursor (Section 2.2). The most relevant information contained in the ^{29}Si NMR spectra shown in Fig. 3 is the presence in the spectra of the functionalized samples of distinctive T^2 and T^3 peaks at about -60 and -69 ppm, respectively. These peaks, which come from silicon atoms in species $R\text{-}Si(OSi)_n(OH)_{3-n}$ ($n=2$, 3), clearly prove functionalization in the NH_2-MCM-41 and COOH-MCM-41 samples. Organic functionalization was also proved by infrared spectroscopy (spectra not shown). Typical ν(C–H) stretching vibrations of the propyl chains at ca. 2900 cm^{-1} and δ(Si–CH_2) bending at 1385 cm^{-1}, together with $\delta(NH_2)$ bending band at ca. 1570 cm^{-1} for the NH_2-MCM-41 sample, and with ν(C=O) stretching band at 1724 cm^{-1} for the COOH-MCM-41 sample, confirmed the presence of organic groups in the functionalized samples. Scanning electron micrographs of MCM-41 spheres after functionalization, and also after cisplatin loading (not shown) confirmed that the spherical shape and particle size was preserved throughout the whole process.

3.2. Cisplatin loading and release

Cisplatin loading was quantified by UV–visible spectroscopy. As stated in Section 2.4, the samples were loaded by immersing them into an aqueous cisplatin solution at 37 °C for 24 h. After this period of time, cisplatin loaded samples

were recovered by filtration, washed with water and dried. The remaining cisplatin solution (to which the sample washing water was added) was analyzed for cisplatin content and, by difference, the cisplatin uptake by the sample was determined. The amount of cisplatin adsorbed (Table 1) by MCM-41C, NH_2-MCM-41C and COOH-MCM-41C samples resulted to be 8.7($\pm$0.7), 61.4($\pm$4.6) and 14.7($\pm$0.6) mg of cisplatin per gram of sample, respectively (all loading measurements were performed in triplicate). These results show a considerable influence of functionalization on cisplatin uptake. Since the pore diameter of the samples under study is in the range of 2.4–3.1 nm and the size of cisplatin molecule is ca. 0.5 nm, diffusion of the drug is unlikely to be the limiting factor for cisplatin uptake. Hence, the differences found in the amount of cisplatin loaded are likely to reflect corresponding differences of interaction energy between the cisplatin molecule and the pore wall, which are expected to depend upon the nature of the corresponding functional group; silanol groups in the case of the unmodified MCM-41, and $-NH_2$ and –COOH groups for the amino and carboxy functionalized samples, respectively.

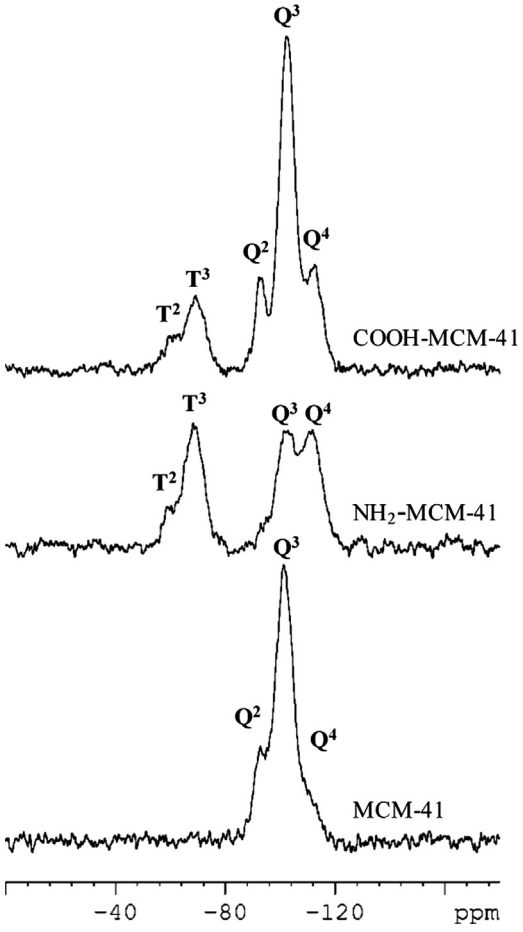

Fig. 3. ^{29}Si MAS NMR spectra of MCM-41, NH_2-MCM-41 and COOH-MCM-41 samples.

The release profiles of cisplatin from the MCM-41 samples are shown in Fig. 4. These in vitro tests were carried out (in triplicate) by immersing 100 mg of cisplatin loaded samples into 50 ml of vigorously stirred saline solution at 37 °C, as stated above. At increasing time, 2 ml of the solution was taken out to quantify the amount of cisplatin released. In order to maintain a constant volume, after each extraction, 2 ml of fresh saline solution was added to the release medium. The MCM-41C sample showed a fast release rate and the plateau corresponding to maximum delivery (37% of the cisplatin loaded) was reached after about 40 h. For the amino-functionalized sample, NH_2-MCM-41C, the release process ends after about 50 h, and only 20% of the loaded cisplatin is released. This shows that the amino functionalized sample retains a higher percentage of the drug. The carboxy-functionalized sample, COOH-MCM-41C, showed a marked capacity to sustain significant drug delivery for about 140 h. This time period is significantly longer than that shown by the other MCM-41 samples reported herein, and also considerably longer than the maximum of 3 days reported by Czarnobaj and Lukasiak [55] for a cisplatin loaded porous silica xerogel. It should be added that Tao et al. [56] have recently reported that pure MCM-41 adsorbs only a negligible amount of cisplatin from a phosphate-buffered solution (PBS) of the drug at pH = 7.4. We avoided the use of such a

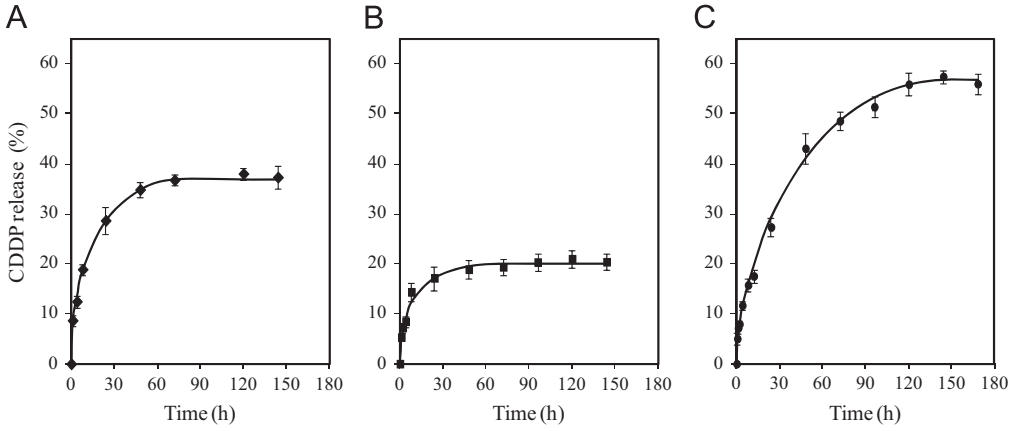

Fig. 4. Release profiles of cisplatin (CDDP) from (A) MCM-41C, (B) NH_2-MCM-41C and (C) COOH-MCM-41C samples (all measurements were made in triplicate). The percentage of the loaded drug being released is plotted as a function of the immersion time of the samples in stirred isotonic NaCl solutions.

buffer because phosphate could adversely affect the stability of cisplatin. However, Table 1 still shows that pure MCM-41 could only be loaded with a much smaller amount of the drug than either NH_2-MCM-41 or COOH-MCM-41; no corresponding studies of functionalized MCM-41 were reported by Tao et al. [56].

The final amount of cisplatin released from the COOH-MCM-41C sample was 57% of the total loaded amount, thus showing the lowest retention of the drug, as compared to MCM-41C and NH_2-MCM-41C. Combination of a higher percentage of released cisplatin with the ability to maintain drug delivery for a longer period, renders the carboxy-functionalized COOH-MCM-41 material a superior carrier for controlled delivery of the chemotherapeutic drug, as compared to the unmodified or to the amino-functionalized NH_2-MCM-41 samples. Since the diameter of the cisplatin molecule (0.5 nm) is, in the three cases investigated, much smaller than the mean pore diameter of the solid carrier (Table 1), the kinetics of drug release is likely to be controlled (mainly) by the magnitude of the interaction forces between the adsorbed molecule and the solid adsorbent, which depends on specific functionalization. In the cisplatin molecule, the Pt(II) ion has two permanently bound amino groups and two labile chloride ligands. The later can easily be replaced by other ligands [57], which in the functionalized MCM-41 porous silicas considered herein would be either the carboxylate functional groups of COOH-MCM-41 or the amino groups in NH_2-MCM-41. Stronger interaction with amino groups than with carboxylate groups (as expected) would explain a larger drug uptake in the case of NH_2-MCM-41 (as seen in Table 1), and also a larger percentage of drug release (after hydrolytic cleavage of the carboxylate bonds) in COOH-MCM-41, as actually found (Fig. 4). At about neutral pH (isotonic NaCl water solution) the maximum release of cisplatin from the COOH-MCM-41C sample was found to be 57% of the total amount of drug loaded, which is (roughly) in agreement with recent results by Gu et al. [41] who studied cisplatin release from carboxyl functionalized MCM-41 as a function of pH, and found that the total released quantity amounted to about 55, 65 and 80% (of the drug loaded) at pH values of 5.5, 6.5 and 7.4, respectively. It is relevant to add that (similar to COOH-MCM-41) carboxylic-acid functionalized periodic mesoporous organosilicas were recently reported [58] to have excellent adsorption capacity towards doxorubicin (another anticancer drug currently commercialized under the trade names of Doxil and Myocet).

4. Conclusions

Sub-micrometric MCM-41 silica spheres were synthesized, functionalized with amino or carboxy groups, and studied as nanoporous carriers for controlled delivery of cisplatin, after due characterization by X-ray diffraction, scanning electron microscopy, nitrogen physisorption and ^{29}Si MAS NMR spectroscopy. Main conclusions from in vitro tests can be summarized as follows:

(1) Pure MCM-41 shows only a small uptake of the drug (9 mg of cisplatin per gram of sample), and hence is not a prospective material for cisplatin delivery.
(2) Both, the amino and the carboxy functionalized MCM-41 samples showed a much greater uptake of the drug than pure MCM-41; a fact that was explained in terms of substitution of amino or carboxylate groups of the functionalized samples for the labile chloride ligands of cisplatin.
(3) The amino functionalized MCM-41 sample showed a greater cisplatin uptake (61 mg per gram) than the carboxy functionalized sample (15 mg per gram); presumably because of a stronger interaction of the drug with amino ligands. However, this stronger interaction also results in a smaller percentage of drug delivery, as compared with the carboxy-functionalized sample: 20 and 57% of the loaded amount, respectively.
(4) Altogether, the carboxy-functionalized MCM-41 sample showed a superior performance as a carrier for controlled delivery of cisplatin on account of, (i) the higher percentage of drug delivered, and (ii) a much more favorable kinetics of the in vitro delivery process, which should facilitate drug delivery control over a significantly longer time period.

Acknowledgments

M.J.V. thanks the Santander Group and the University of the Balearic Islands for a Ph.D. fellowship.

References

[1] D.J. Sonneveld, H.J. Hoekstra, W.T. van der Graaf, W.J. Sluiter, N.H. Mulder, P.H. Willemse, H.S. Hoops, D.T. Slejfer, Improved long term survival of patients with metastatic nonseminomatous testicular germ cell carcinoma in relation to prognostic classification systems during the cisplatin era, Cancer 91 (2001) 1304.
[2] R.H. Jones, P.A. Vasey, Part II: testicular cancer-management of advanced disease, Lancet Oncology 4 (2003) 738.
[3] J. Li, Q. Feng, J.M. Kim, D. Schneiderman, P. Liston, M. Li, B. Vanderhyden, W. Faught, M.F.K. Fung, M. Senterman, R.G. Korneluk, B.K. Tsang, Human ovarian cancer and cisplatin resistance: possible role of inhibitor of apoptosis proteins, Endocrinology 142 (2008) 370.
[4] D.K. Armstrong, B. Bundy, L. Wenzel, H.Q. Huang, R. Baergen, S. Lele, L.J. Copeland, J.L. Walker, R.A. Burger, Intraperitoneal cisplatin and paclitaxel in ovarian cancer, New England Journal of Medicine 354 (2006) 34.
[5] P.G. Rose, B.N. Bundy, E.B. Watkins, J.T. Thigpen, G. Deppe, M.A. Maiman, D.L. Clarke-Pearson, S. Insalaco, Concurrent cisplatin-based radiotherapy and chemotherapy for locally advanced cervical cancer, New England Journal of Medicine 340 (1999) 1144.
[6] D.R. Scribner, D.M. Benbrook, Retinoids enhance cisplatin-based chemoradiation in cervical cancer cells in vitro, Gynecologic Oncology 85 (2002) 223.
[7] D.H. Johnson, Locally advanced, unresectable non-small cell lung cancer: new treatment strategies, Chest 117 (2000) 1335.
[8] W.G. Deng, G. Wu, K. Ueda, K. Xu, J.A. Roth, L. Ji, Enhancement of antitumor activity of cisplatin in human lung cancer cells by tumor suppressor FUS1, Cancer Gene Therapy 15 (2008) 29.

[9] A.K. Nowak, M.J. Byrne, R. Willianson, G. Ryan, A. Segal, D. Fielding, P. Mitchell, A.W. Musk, B.W.S. Robinson, A multicentre phase II study of cisplatin and gemcitabine for malignant mesothelioma, British Journal of Cancer 87 (2002) 491.
[10] A. Santoro, M.E. O'Brien, R.A. Stahel, K. Nackaerts, P. Baas, M. Karthaus, W. Eberhardt, L. Paz-Ares, S. Sundstrom, Y. Liu, V. Ripoche, J. Blatter, C.M. Visseren-Grul, C. Manegold, Pemetrexed plus cisplatin or pemetrexed plus carboplatin for chemonaïve patients with malignant pleural mesothelioma: results of the International Expanded Access Program, Journal of Thoracic Oncology 3 (2008) 756.
[11] M.P. Goren, R.K. Wright, M.E. Horowitz, Cumulative renal tubular damage associated with cisplatin nephrotoxicity, Cancer Chemotherapy and Pharmacology 18 (1986) 69.
[12] S.D. Schaefer, J.D. Post, L.G. Close, C.G. Wright, Ototoxicity of low- and moderate-dose cisplatin, Cancer 56 (1985) 1934.
[13] R.R. Reddel, R.F. Kefford, J.M. Grant, A.S. Coates, R.M. Fox, M.H. Tattershall, Ototoxicity in patients receiving cisplatin: importance of dose and method of drug administration, Cancer Treatment Reports 66 (1982) 19.
[14] E. Wong, C.M. Giandomenico, Current status of platinum-based antitumor drugs, Chemical Reviews 99 (1999) 2451.
[15] J.H. Kim, J.I. Lim, H.-K. Park, Porous chitosan-based adhesive patch filled with poly(l-3,4-dihydroxyphenylalanine) as a transdermal drug-delivery system, Journal of Porous Materials 20 (2013) 177–182.
[16] Y.-H. Kim, I.-K. Kim, T.-G. Kim, J.-H. Lee, Y.-K. Lim, Y.-J. Kim, S.-Y. Choi, Sustained drug release system using porous structured poly(l-lactic acid) fabricated by solvent dispersion method, Journal of Porous Materials 20 (2013) 303–308.
[17] S. Ramachandran, A.P. Quist, S. Kumar, R. Lal, Cisplatin nanoliposomes for cancer therapy: AFM and fluorescence imaging of cisplatin encapsulation, stability, cellular uptake, and toxicity, Langmuir 22 (2006) 8156.
[18] P. Utreja, S. Jain, A.K. Tiwary, Localized delivery of paclitaxel using elastic liposomes: formulation development and evaluation, Drug Delivery 18 (2011) 367–376.
[19] M. Vallet-Regí, F. Balas, D. Arcos, Mesoporous materials for drug delivery, Angewandte Chemie International Edition 46 (2007) 7548.
[20] M. Öner, E. Yetiz, E. Ay, U. Uysal, Ibuprofen release from porous hydroxyapatite tablets, Ceramics International 37 (2011) 2117–2125.
[21] B. Colovic, S. Pasalic, V. Jokanovic, Influence of hydroxyapatite pore geometry on tigecycline release kinetics, Ceramics International 38 (2012) 6181–6189.
[22] M. Betsiou, G. Bantsis, I. Zoi, C. Sikalidis, Adsorption and release of gemcitabine hydrochloride and oxaliplatin by hydroxyapatite, Ceramics International 38 (2012) 2719–2724.
[23] J. Lu, M. Liong, S. Sherman, T. Xia, M. Kokochich, A.E. Nel, J.I. Zink, F. Tamanoi, Mesoporous silica nanoparticles for cancer therapy: energy-dependent cellular uptake and delivery of paclitaxel to cancer cells, Nanobiotechnology 3 (2007) 89.
[24] S. Giri, B.G. Trewyn, V.S.Y. Lin, Mesoporous silica nanomaterial-based biotechnological and biomedical delivery systems, Nanomedicine 2 (2007) 99.
[25] K.K. Cotí, M.E. Belowich, M. Liong, M.W. Ambrogio, Y.A. Lau, H.A. Khatib, J.I. Zink, N.M. Khashab, J.F. Stoddart, Mechanised nanoparticles for drug delivery, Nanoscale 1 (2009) 16.
[26] J.L. Vivero-Escoto, I.I. Slowing, B.G. Trewyn, V.S.Y. Lin, Mesoporous silica nanoparticles for intracellular controlled drug delivery, Small 6 (2010) 1952.
[27] M. Vallet-Regi, M. Colilla, B. Gonzalez, Medical applications of organic–inorganic hybrid materials within the field of silica-based bioceramics, Chemical Society Reviews 40 (2011) 596.
[28] S.H. Wu, Y. Hung, C.Y. Mou, Mesoporous silica nanoparticles as nanocarriers, Chemical Communications 47 (2011) 9972.
[29] V. Cauda, L. Muhlstein, B. Onida, T. Bein, Tuning drug uptake and release rates through different morphologies and pore diameters of confined mesoporous silica, Microporous and Mesoporous Materials 118 (2009) 435.
[30] E. Ghedini, M. Signoretto, F. Pinna, V. Crocella, L. Bertinetti, G. Cerrato, Controlled release of metoprolol tartrate from nanoporous silica matrices, Microporous and Mesoporous Materials 132 (2010) 258.
[31] H. Wang, X. Gao, Y. Wang, J. Wang, X. Niu, X. Deng, Effect of amine functionalization of SBA-15 on controlled baicalin drug release, Ceramics International 38 (2012) 6931–6935.
[32] Z. Li, J.C. Barnes, A. Bosoy, J.F. Stoddart, J.I. Zink, Mesoporous silica nanoparticles in biomedical applications, Chemical Society Reviews 41 (2012) 2590.
[33] R. Vathyam, E. Wodimu, S. Das, C. Zhang, S. Hayes, Z. Tao, T. Asefa, Improving drug adsorption and release properties on nanostructured materials with temperature, Journal of Physical Chemistry C 115 (2011) 13135.
[34] N. Linares, E. Serrano, M. Rico, A.M. Balu, E. Losada, R. Luque, J. Garcia-Martinez, Incorporation of chemical functionalities in the framework of mesoporous silica, Chemical Communications 47 (2011) 9024.
[35] I.I. Slowing, L. Vivero-Escoto, C.W. Wu, V.S.Y. Lin, Mesoporous silica nanoparticles as controlled release drug delivery and gene transfection carriers, Advanced Drug Delivery Reviews 60 (2008) 1278.
[36] D. Quintanar-Guerrero, D. Ganem-Quintanar, M.G. Nava-Arzaluz, E. Piñon-Segundo, Silica xerogels as pharmaceutical drug carriers, Expert Opinion on Drug Delivery 6 (2009) 485.
[37] M. Al Shamsi, M.T. Al Samri, S. Al-Salam, W. Conca, S. Shaban, S. Benedict, S. Tariq, A.V. Biradar, H.S. Penefsky, T. Asefa, A.K. Souid, Biocompatibility of calcined mesoporous silica particles with cellular bioenergetics in murine tissues, Chemical Research in Toxicology 23 (2010) 1796.
[38] J. Lu, M. Liong, Z. Li, J.I. Zink, F. Tamanoi, Biocompatibility, biodistribution, and drug-delivery efficiency of mesoporous silica nanoparticles for cancer therapy in animals, Small 16 (2010) 1794.
[39] M. Colilla, B. González, M. Vallet-Regí, Mesoporous silica nanoparticles for the design of smart delivery nanodevices, Biomaterials Science 1 (2013) 114–134.
[40] M.D. Popova, A. Szegedi, I.N. Kolev, J. Mihaly, B.S. Tzankov, G.T. Momekov, N.G. Lambov, K.P. Yoncheva, Carboxylic modified spherical mesoporous silicas as drug delivery carriers, International Journal of Pharmaceutics 43 (2012) 778–785.
[41] J. Gu, S. Su, Y. Li, Q. He, J. Zhong, J. Shi, Surface modification–complexation strategy for cisplatin loading in mesoporous nanoparticles, Journal of Physical Chemistry Letters 1 (2010) 3446–3450.
[42] M. Manzano, V. Aina, C.O. Arean, F. Balas, V. Cauda, M. Colilla, M.R. Delgado, M. Vallet-Regí, Studies on MCM-41 mesoporous silica for drug delivery: effect of particle morphology and amine functionalization, Chemical Engineering Journal 137 (2008) 30.
[43] M. Grün, I. Lauer, K.K. Unger, The synthesis of micrometer- and submicrometer-size spheres of ordered mesoporous oxide MCM-41, Advanced Materials 9 (1997) 254.
[44] W. Stöber, A. Fink, E. Bohn, Controlled growth of monodisperse silica spheres in the micron size range, Journal of Colloid and Interface Science 26 (1968) 62.
[45] T. Yokoi, H. Yoshitake, T. Tatsumi, Synthesis of amino-functionalized MCM-41 via direct co-condensation and post-synthesis grafting methods using mono-, di- and tri-amino-organoalkoxysilanes, Journal of Materials Chemistry 14 (2004) 951.
[46] M.R. Mello, D. Phanon, G. Gleiciani, P. Llewellyn, C. Ronconi, Amine-modified MCM-41 mesoporous silica for carbon dioxide capture, Microporous and Mesoporous Materials 143 (2011) 174.
[47] E.D. Golla, G.H. Ayres, Spectrophotometric determination of platinum with o-phenylenediamine, Talanta 20 (1973) 199.
[48] J.S. Beck, J.C. Bartuli, J.W. Roth, M.E. Lenowicz, C.T. Kresge, K.D. Schimtt, C.T.W. Chu, D.H. Olson, E.W. Sheppard, S.B. McCullen, J.B. Higgins, J.L. Schlenker, A new family of mesoporous molecular sieves prepared with liquid crystal templates, Journal of the American Chemical Society 114 (1992) 10834.

[49] B. Onida, B. Bonelli, L. Flora, F. Geobaldo, C. Otero Arean, E. Garrone, Permeability of micelles in surfactant-containing MCM-41 silica as monitored by embedded dye molecules, Chemical Communications 21 (2001) 2216.
[50] A. Rámila, B. Muñoz, J. Pérez-Pariente, M. Vallet-Regí, Mesoporous MCM-41 as drug host system, Journal of Sol–Gel Science and Technology 26 (2003) 1199.
[51] S.W. Song, K. Hidajat, S. Kawi, Functionalized SBA-15 materials as carriers for controlled drug delivery: influence of surface properties on matrix–drug interactions, Langmuir 21 (2005) 9568.
[52] M. Kruk, M. Jaroniec, A. Sayari, Relations between pore structure parameters and their implications for characterization of MCM-41 using gas adsorption and X-ray diffraction, Chemistry of Materials 11 (1999) 492.
[53] M. Jaroniec, M. Kruk, H.J. Shin, R. Ryoo, Y. Sakamoto, O. Terasaki, Comprehensive characterization of highly ordered MCM-41 silicas using nitrogen adsorption, thermogravimetry, X-ray diffraction and transmission electron microscopy, Microporous and Mesoporous Materials 48 (2001) 127.
[54] P.I. Ravikovitch, S.C.O. Domhnaill, A.V. Neimark, F. Schuth, K.K. Unger, Capillary hysteresis in nanopores: theoretical and experimental studies of nitrogen adsorption on MCM-41, Langmuir 11 (1995) 4765.
[55] K. Czarnobaj, J. Lukasiak, In vitro release of cisplatin from sol–gel processed porous silica xerogels, Drug Delivery 11 (2004) 341.
[56] Z. Tao, Y. Xie, J. Goodisman, T. Asefa, Isomer-dependent adsorption and release of cis- and trans-platin anticancer drugs by mesoporous silica nanoparticles, Langmuir 26 (2010) 8914–8924.
[57] V.T. Huynh, P. de Souza, M.H. Stenzel, Polymeric micelles with pendant dicarboxylato chelating ligands prepared via a Michael addition for cis-platinum drug delivery, Macromolecules 44 (2011) 7888–7900.
[58] H.M. Kao, C.H. Chung, D. Saikia, S.H. Liao, P.Y. Chao, Y.H. Chen, K.C.W. Wu, Highly carboxylic-acid-functionalized ethane-bridged periodic mesoporous organosilicas: synthesis, characterization, and adsorption properties, Chemistry—An Asian Journal 7 (2012) 2111–2117.